Angle-resolved electron spectra in short-pulse two-color XUV + IR photoionization of atoms

A. K. Kazansky,[1,2] I. P. Sazhina,[3] and N. M. Kabachnik[2,3,4]

[1]*V. A. Fock Institute of Physics, State University of Sankt Petersburg, Sankt Petersburg 198504, Russia*

[2]*Donostia International Physics Center, E-20018 San Sebastian/Donostia, Basque Country, Spain*

[3]*Institute of Nuclear Physics, Moscow State University, Moscow 119991, Russia*

[4]*Institute of Theoretical Physics, University of Hamburg, D-20355 Hamburg, Germany*

(Received 16 June 2010; published 20 September 2010)

Spectra and angular distributions of photoelectrons from ionization of atoms by a combination of two short pulses in the XUV and IR range are theoretically considered. The transition from the streaking regime for ultrashort XUV pulses to the sideband formation for longer pulses is discussed. For photoelectrons of sufficiently high energy (a few hundreds of eV), the peculiarity of the angular distribution and the gross structure of the sidebands are investigated.

DOI: 10.1103/PhysRevA.82.033420 PACS number(s): 32.80.Fb, 32.80.Rm, 42.65.Re

I. INTRODUCTION

With the advent of free-electron lasers (FEL) in the extreme ultraviolet (XUV) and x-ray regions, and of new XUV sources based on high-order harmonic generation (HHG), the experiments with synchronized XUV and infrared (IR) pulses from powerful lasers have received a special attention. Studies of the two-color XUV + IR photoionization can provide fundamental information on the properties of the continuum spectrum of atoms and molecules and on the so-called free-free transitions (see, for example, Ref. [1] and references therein). Moreover, such experiments can be used to study the properties of the FEL radiation [2] and of the harmonics in HHG [3].

When a photoelectron is produced by an XUV pulse in the presence of a laser pulse, the electron energy can be changed due to interaction with the electromagnetic field of the laser. Depending on the characteristics of the pulses, there are different scenarios of the process. The basic parameters which determine the character of the process are the durations of the XUV and the IR pulses, τ_X and τ_L, respectively, and the period of the laser field T_L. If $\tau_X \ll T_L$, the created pulse of photoelectrons (replica of the XUV pulse) is extremely short and all electrons appear in the laser field practically at the same phase. This is a typical case of the conventional streaking effect [4,5] which was widely used for characterization of the attosecond XUV pulses [6–8] and very recently also of the FEL femtosecond pulses [9]. Similar conditions are fulfilled for each individual pulse in experiments with the trains of attosecond pulses [10,11].

In another limiting case of the laser assisted photoelectric effect (LAPE) when $\tau_L > \tau_X \gg T_L$, specific structures at the wings of a photoline, the so-called sidebands, appear. The sidebands consist of a regular sequence of lines with the interval between lines equal to the laser photon energy. They were studied experimentally [12–15] as well as theoretically [16–18].

Quite informative is the study of angular distributions of photoelectrons in the two-color photoionization. The angle resolved studies of XUV + IR atomic photoionization have been reported in both regimes: sideband formation in ionization by high-order harmonics [19,20] and ionization of atoms by a train of attosecond pulses in the presence of a strong IR laser field [21,22]. It was demonstrated that the angular distributions are sensitive to the time delay between the XUV and IR pulses and to the relative phases and intensities of the harmonics. All these studies were made for comparatively low energy of emitted photoelectrons (below 20 eV). In such conditions the photoelectron spectrum contains a few sidebands and their angular distribution is simple, determined mainly by the dipole selection rule in absorption of one-two photons.

Much less attention has been devoted to the intermediate case when $\tau_X \approx T_L$. Nowadays, this case becomes of a special interest for the experiments with the new x-ray FEL facilities such as the Linac coherent light source [23]. Here the duration of the XUV pulse can be smaller than 10 fs [24], i.e., it covers only two to four periods of the IR field, which has a period typically $T_L \approx 2.7$ fs for a Ti:sapphire laser operated at 800 nm. A study of the intermediate case is important for understanding the mechanism of formation of the sidebands. Moreover, the large energy of generated photons at an x-ray FEL permits one to study peculiarities of the sidebands at high kinetic energies where strong irregularity of the sideband intensity can be expected.

Theoretically the two-color photoionization of atoms have been considered in numerous articles using various theoretical technique. The simplest approach is based on the strong-field approximation (SFA) [25] which was successfully used both in the streaking regime [5,26] and in the conditions of sideband formation (see, e.g., Refs. [1,16]). More refined treatment includes the interaction of the emitted electron with the Coulomb field of the residual ion (see Refs. [16,27,28] and references therein for earlier articles). More sophisticated theories are based on a numerical solution of time-dependent Schrödinger equation (see, for example, Refs. [17,18,20,26,29,30]).

The aim of this work is twofold. First, we investigate the transition from the streaking to the sideband regime paying a special attention to the formation of the sideband structure. Second, having in mind application at an x-ray FEL, we analyze the case of high-energy photoelectrons, when the number of sidebands is large. Here we investigate the angular dependence and the gross structure of the sideband spectrum. We use the simplest description of the process, namely the SFA and a single-active-electron approach. Earlier, a similar

problem was considered for the case of laser-assisted Auger decay [31–33]. We note that within the strong-field approximation used in our analysis, there is a close analogy between the formation of sidebands in photoelectron and Auger-electron spectra. In both cases the sidebands appear due to interaction of the emitted electron with the IR laser field, whereas the physical mechanism of the electron ejection plays a secondary role. In spite of this similarity, we believe that a special analysis of the two-color XUV + IR photoionization by short pulses is necessary for proper interpretation of experimental results. First such experiments have been already realized [2,15]. It is clear that also in the future they will be performed for characterization of the pulses generated by new FELs. A study of the sideband structure is the first and necessary element of the analysis of such experiments. In comparison with the Auger decay, the case of XUV + IR photoionization has an advantage that the duration of the electron pulse, which is determined by the duration of the XUV pulse, can be varied while the equivalent duration of the Auger electron emission is determined by the lifetime of the Auger state. In addition, it is easier to study the sidebands in laser-assisted photoionization than in the Auger decay. In the latter case many Auger lines are excited and their sidebands overlap, which makes spectral analysis more complicated [34]. Finally we note that due to different selection rules in photoemission and Auger emission, the angular distributions of the sidebands should differ substantially in these two cases. Thus the angle resolved sideband structure in photoemission of energetic electrons deserves a special theoretical investigation.

II. BASIC EQUATIONS AND APPROXIMATIONS

Using a standard approach to the laser assisted XUV photoionization of an atom [35,36] we consider the process within the first-order time-dependent perturbation theory [37]. The amplitude of the transition from the initial state $\Psi_0 \exp(-iE_0t)$ to the final state which contains the ionic state $\Psi_f \exp(-iE_ft)$ and the emitted photoelectron state $\psi_{\vec{k}}$ may be written using the length gauge as follows (atomic units are used throughout unless otherwise indicated):

$$\mathcal{A}_{\vec{k}} = -i \int_{-\infty}^{\infty} dt\ \bar{\mathcal{E}}_X(t) \langle \Psi_f \psi_{\vec{k}} | \hat{D} | \Psi_0 \rangle \exp[i(E_b - \omega_X)t], \tag{1}$$

where $\bar{\mathcal{E}}_X(t)$ is the envelope of the XUV pulse, ω_X is its carrier frequency, $\hat{D}$ is the dipole operator, and $E_b = E_f - E_0$ is the binding energy (positive) of the electron. The wave function $\psi_{\vec{k}}(t)$ describes the "dressed" photoelectron in the laser field, which is characterized by the final (asymptotic) momentum $\vec{k}$. The following consideration is based on the SFA [25] in which the wave function of the photoelectron is represented by the nonrelativistic Volkov wave function [38]:

$$\psi_{\vec{k}} = \exp\{i[\vec{k} - \vec{A}_L(t)]\vec{r} - i\Phi(\vec{k},t)\}. \tag{2}$$

Here

$$\Phi(\vec{k},t) = \frac{1}{2}\int_t^{\infty} dt'[\vec{k} - \vec{A}_L(t')]^2 \tag{3}$$

with $\vec{A}_L(t)$ being the vector potential of the laser field, which we define as $\vec{A}_L(t) = \int_t^{\infty} dt' \vec{\mathcal{E}}_L(t')$ where $\vec{\mathcal{E}}_L(t)$ is the IR laser electric field vector. (We assume that both XUV and IR fields are linearly polarized along the same direction which is chosen as the z axis of the coordinate system.) Moreover, we ignore the influence of the laser field on the bound ionic and atomic states which is a sufficiently good approximation for not very strong laser fields (10^{12}–10^{13} W/cm^2) considered here.

Equation (1) can be interpreted in this way: at moment t an electron is created by the XUV field with momentum $\vec{k}_0$ which is then transferred by the IR field to the final state with momentum $\vec{k}$. Since $\vec{k}$ is fixed, this means that $\vec{k}_0 = \vec{k} - \vec{A}_L(t)$ depends on t.

The transverse momentum is conserved, thus

$$k_0 \sin\vartheta_0 = k \sin\vartheta, \tag{4}$$

where ϑ_0 is the angle of electron emission from atom in the laser field and ϑ is the angle of photoemission (at infinity). The modulus of the momenta are connected by the relation:

$$\frac{k_0^2(t)}{2} = \frac{k^2}{2} - kA(t)\cos\vartheta + A^2(t)/2. \tag{5}$$

Substituting Eq. (2) into Eq. (1) and using the single-active-electron approximation one can reduce the dipole matrix element in Eq. (1) to the single-electron photoionization amplitude, $d_{\vec{k}_0}$, which after expansion in partial waves may be presented as

$$d_{\vec{k}_0} = d_{l_0-1}[Y_{l_0-1,m_0}(\vartheta_0,0) + R\, e^{i(\delta_{l_0+1}-\delta_{l_0-1})} Y_{l_0+1,m_0}(\vartheta_0,0)], \tag{6}$$

where $d_{l_0\pm1}$ are the partial dipole amplitudes for the transitions from the initial state with the orbital angular momentum l_0, Y_{lm} are spherical harmonics, $R = |d_{l_0+1}|/|d_{l_0-1}|$, and $\delta_{l_0\pm1}$ are the photoionization phases. If $l_0 = 0$ (s shell), the amplitude is

$$d_{\vec{k}_0} = d_s Y_{1,0}(\vartheta_0,0). \tag{7}$$

Further in this section we consider s shell ionization.

We are interested in the region of rather large energies of photoelectrons (hundreds of eV) when the sidebands consist of many lines, whereas the spread of the sideband structure is much smaller than the photoelectron energy. Since at large energies the dipole matrix element depends weakly on the energy, one can ignore its energy dependence. Then the amplitude of s shell photoionization may be approximated as

$$\mathcal{A}_{\vec{k}} \approx -id_s\mathcal{F}_a(\vec{k}), \tag{8}$$

where the function $\mathcal{F}_a(\vec{k})$ is defined as

$$\mathcal{F}_a(\vec{k}) = \int_{t_0}^{t_M} dt\ \bar{\mathcal{E}}_X(t) Y_{1,0}(\vartheta_0(t),0) \times \exp\left[i\int_t^{\infty} dt' \left(\frac{1}{2}[k^2 - 2kA_L(t')\cos\vartheta + A_L^2(t')] - \frac{1}{2}\kappa^2\right)\right], \tag{9}$$

where t_0 and t_M correspond to the beginning and the end of the XUV pulse, respectively, and $\kappa^2/2 = \omega_X - E_b$ is the energy of the electron ejected by a very long pulse in absence of the

IR field. Here and in the following the XUV pulse is supposed to be shorter than the laser pulse and it completely overlaps with the latter. In order to evaluate $\mathcal{F}_a(\vec{k})$ one should calculate $\vartheta_0(t)$ for each pair (k,ϑ) and then integrate over t.

The value $|\mathcal{F}_a|^2$ represents the spectrum of photoelectrons in the laser field. If the XUV pulse is very short ($\tau_X \ll T_L$), the vector potential $\vec{A}_L$ is practically constant during the XUV pulse, $\vec{A}_L(t_0)$, and the function $\mathcal{F}_a(\vec{k})$ is proportional to the δ function $\delta([\vec{k} - \vec{A}_L(t_0)]^2 - \kappa^2)$. This gives the known picture of streaking [4], namely the photoelectron peak is shifted by the laser field from its original position $\kappa^2/2$ to the new one determined by the value of the vector potential at the moment of photoemission.

In the opposite case, when the pulses are infinitely long, one can obtain, by supposing $\vec{A}_L(t) = \vec{A}_{0L}\sin\omega_L t$ and ignoring the term proportional to A_L^2 in Eq. (9), the well-known result that the spectrum consists of sideband lines at the energies of $k_n^2 = \kappa^2 \pm 2n\omega_L$, with the intensity proportional to the square of Bessel function $J_n^2(\vec{A}_{0L}\cdot\vec{k}_n/\omega_L)$ (this case is discussed in detail in Ref. [1]). If the quadratic term in $A_L(t)$ is retained in Eq. (9), the integral can be expressed in terms of the generalized Bessel functions [39] $J_n(\alpha,\beta)$.

Our goal is to analyze the intermediate case when the XUV pulse duration is equal to a few periods of the IR field. In the following we first present several examples of the spectra obtained by numerical calculation of $|\mathcal{F}_a(\vec{k})|^2$ and then analyze this factor analytically.

III. RESULTS AND DISCUSSION

A. Photoelectron spectra

Using Eq. (9), we have calculated the photoelectron spectra from laser-assisted photoionization generated by the XUV pulses of various duration. In this section we suppose that the photoelectron is emitted along the polarization vector of the laser field. The energy of the photoelectron without IR field is set equal to 220 eV (8.09 a.u.). The laser field has parameters frequently used in experiments: the photon energy is 1.66 eV (the carrier wavelength is ~800 nm), the pulse duration is 20 fs, and the intensity is 3.5×10^{12} W/cm^2 (the electric field amplitude is about 0.01 a.u.). The results of our calculations are presented in Fig. 1. Different panels show the calculated spectra for different durations of the XUV pulse which is supposed to have a Gaussian shape. The laser pulse envelope has a flat central part with sharp increase at the beginning and decrease at the end of the pulse. In the insets we show the vector potential of the IR field and the envelope of the XUV pulse in arbitrary units (the pulses are plotted as normalized to the same maximum value). We have assumed that the maximum of the Gaussian XUV pulse is at the middle of the IR pulse and coincides with one of the maxima of its vector potential. The vertical dashed line in all figures shows the position of the photoelectron energy in the absence of the laser field.

In Fig. 1(a), the duration of the XUV pulse (FWHM of the field) is 1 fs. This is close to the half period of the laser field ($T_L = 2.5$ fs). The photoelectron spectrum consists of a big maximum at the energy ~8.7 a.u. (236 eV) which is shifted from the original energy 220 eV due to the streaking effect. In addition, there are smaller maxima at the low-energy side which are due to interference of electrons emitted at different moments of the IR pulse. Since the energy difference between these maxima is not a constant and it is not equal to the frequency of the laser field, the maxima are not the usual sidebands. A very similar picture has been obtained in our article [26] by solving numerically the time-dependent Schrödinger equation which describes the photoionization of Ar($3s$) subshell. We note that if the position of the XUV pulse is shifted by one-half of the IR period, the main maximum will be shifted to the lower energy (~7.5 a.u.) and the whole spectrum will be a mirror reflection of the presented one with respect to the unperturbed photoline position. For even smaller duration of the XUV pulse the small peaks gradually disappear, and the spectrum contains only the main peak at shifted position which depends on the delay time between pulses (streaking).

Figure 1(b) presents the results for the XUV pulse of 2 fs duration. In this case, a large part of the pulse overlaps with the other half-periods of the IR vector potential (see insert). Correspondingly, in the low-energy part of the spectrum strong lines appear. They are separated by the energy interval of about 1.6 eV (0.06 a.u.), which corresponds to the energy of the IR quanta.

When the XUV pulse duration is larger (3 fs), the main (right) peak also reveals the structure with the interval of 1.6 eV [see Fig. 1(c)]. The spectrum becomes more symmetric with respect to the original energy of 220 eV. This tendency continues in Fig. 1(d) which corresponds to the XUV pulse of 4-fs width. Further increase of the XUV pulse duration does not lead to a qualitative change of the spectrum. The lines become narrower and higher, but new lines do not appear.

Inspecting Fig. 1(d), one notes that the variation of the sideband intensity is not regular, but the lines exhibit some gross structure. Similar gross structure was revealed also in laser-assisted Auger electron spectra [33]. In order to make the gross structure clearly visible we have averaged the spectrum by convoluting it with a Gaussian function with the width (FWHM) of ~2 eV, larger than the spacing of the sideband lines. This Gaussian averaging imitates the experimental resolution. The resulting curves are shown in all four panels by the thick (red) lines. Interestingly, the positions of the maxima and minima of the curves are very robust and are almost independent of the duration of the XUV pulse.

In order to explain the behavior of the sideband spectra for different pulse widths and the origin of the gross structure we have analyzed the basic expression (9) following the lines suggested in Ref. [33]. For convenience, we suppose that both the XUV and the IR pulses are almost flat with a sharp increase of the intensity at the beginning and a steep decrease at the end of the pulse. In this case, to a rather good approximation, the value of the IR pulse vector potential can be expressed as $A_L(t) = \alpha + A_{0L}\sin\omega_L t$, where the constant α is determined by the contribution to $\vec{A}_L(t)$ from the rear part of the pulse where its intensity decreases to zero, and A_{0L} is the amplitude of the vector potential. We assume that $t = 0$ is chosen at the beginning of the XUV pulse ($t_0 = 0$), thus $A_L(t_0) = \alpha$. Let consider the case when the IR pulse is longer than XUV pulse, so the XUV pulse covers only a few oscillations of the laser

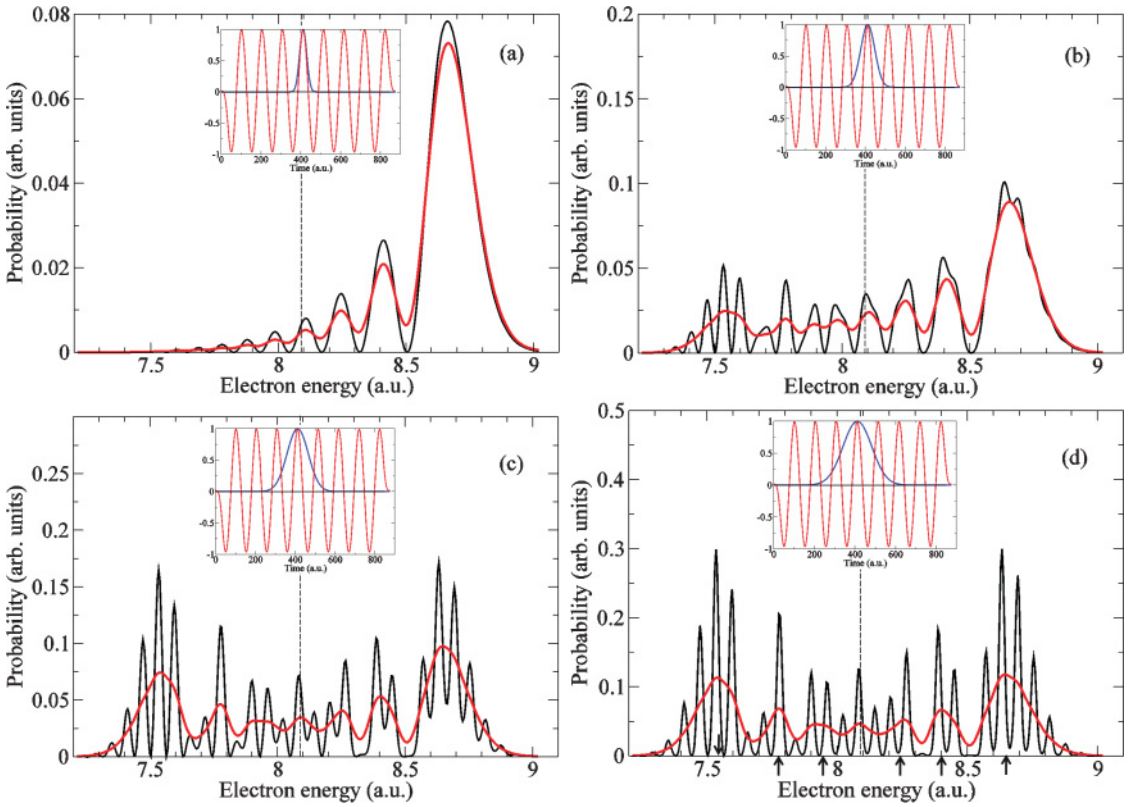

FIG. 1. (Color online) The calculated electron spectra (thin black lines) excited by the XUV pulses of different durations [(a) 1 fs, (b) 2 fs, (c) 3 fs, (d) 4 fs] in the field of the 3.5×10^{12} W/cm^2 IR laser. The duration of the laser pulse is 20 fs. In the inserts the vector potential of the IR and the envelope of the XUV pulses are shown. For further details see text. Thick (red) lines show the averaged spectra. Dashed vertical line shows the position of the unperturbed photoline.

field. Then the integral (9) can be approximated by a sum of contributions of time intervals equal to the period of the laser pulse:

$$\mathcal{F}(k) \approx \sum_{n=1}^{N_{\max}} E_n(k)[J(k)]^n, \tag{10}$$

where $N_{\max} = \tau_X / T_L$ is the number of full periods of the laser field covered by the XUV pulse,

$$J(k) = \exp\left(i \int_0^{T_L} dt'' \frac{1}{2}\{[k - A_L(t'')]^2 - \kappa^2\} \right), \tag{11}$$

and

$$E_n(k) = \int_{(n-1)T_L}^{nT_L} dt' \bar{\mathcal{E}}_X(t') \times \exp\left(i \int_{(n-1)T_L}^{t'} dt'' \frac{1}{2}\{[k - A_L(t'')]^2 - \kappa^2\} \right). \tag{12}$$

Since $\bar{\mathcal{E}}_X(t)$ is almost constant during the pulse $\bar{\mathcal{E}}_X(t) \sim \mathcal{E}_{0X}$, and since $A_L(t)$ is a periodic function within the IR pulse, the value $E_n(k)$ is approximately constant, independent of n. It may be presented as

$$E_n(k) \approx \tilde{E}(k) = \mathcal{E}_{0X} \int_0^{T_L} dt e^{iQ(t)}, \tag{13}$$

where

$$Q(t) = \int_0^t dt' \frac{1}{2}\{[k - A_L(t')]^2 - \kappa^2\}. \tag{14}$$

In this case the sum in Eq. (10) can be computed:

$$\mathcal{F}(k) \approx \tilde{E}(k) \frac{1 - [J(k)]^{N_{\max}+1}}{1 - J(k)}. \tag{15}$$

There are two types of structure in the spectrum, presented by Eq. (15): the narrow structure determined by the condition $J(k) = 1$, where the quantity $\mathcal{F}(k) \approx \tilde{E}(k) N_{\max}$, and the broader structure associated with the k dependence of the quantity $\tilde{E}(k)$. The structure of the first type consists of narrow peaks with the spacing between them close to the IR frequency. The structure of the second type is a modulation of the amplitudes of the narrow peaks. This is a gross structure which reveals itself in the energy averaged spectra. It can be qualitatively described using the stationary phase approach. We note that the value $\tilde{E}(k)$ within a factor coincides with the value $G(t_X + T_L)$ for $t_X = 0$ considered in the Appendix of Ref. [33]. As it was shown in that article, the main contribution to the integral (12) comes from the region around the stationary phase points t_s which are determined by the equation

$$k - A_L(t_s) = \pm\kappa, \tag{16}$$

where the plus (minus) sign corresponds to the ejection of electrons in (opposite to) the direction of the IR field. Note that

this confirms the validity of our assumption of factorization of the amplitude (8), since the dipole amplitude can be taken at $k = \kappa$. Within the stationary phase approximation the value $\tilde{E}(k)$ can be presented [33] in terms of Airy functions as follows:

$$\tilde{E}(k) \approx \mathcal{E}_{0X} \times \begin{cases} e^{iQ(t_{\max})} \left[\frac{8\pi^2|S|^{1/2}}{\kappa|\mathcal{E}_L(t_s)|}\right]^{1/2} \mathrm{Ai}(S) \\ \quad \text{if} \quad k > \alpha + \kappa, \\ e^{iQ(t_{\min})} \left[\frac{8\pi^2|\bar{S}|^{1/2}}{\kappa|\mathcal{E}_L(t_s)|}\right]^{1/2} \mathrm{Ai}(\bar{S}) \\ \quad \text{if} \quad k < \alpha + \kappa, \end{cases} \tag{17}$$

where the Airy function $\mathrm{Ai}(z)$ is defined as in Ref. [40] and

$$S = \frac{\left[(k-\alpha-A_0)^2 - \kappa^2\right]}{[4A_0\omega_L^2(k-\alpha-A_0)]^{1/3}}, \tag{18}$$

$$\bar{S} = \frac{\left[(k-\alpha+A_0)^2 - \kappa^2\right]}{[-4A_0\omega_L^2(k-\alpha+A_0)]^{1/3}}. \tag{19}$$

In Eq. (17) t_s is the stationary phase point which is determined by Eq. (16). The phases $Q(t_{\max})$ and $Q(t_{\min})$ are calculated according to Eq. (14) for the points $t_{\max}$ and $t_{\min}$, where the vector potential reaches its maximal and minimal values, respectively (for more details see the Appendix in Ref. [33]). As follows from Eq. (17), the maxima and minima in the gross structure, that is described by the modulus squared $|\tilde{E}(k)|^2$, are determined by the extrema and zeros of the Airy function, respectively. Asymptotically the Airy function is presented as [40]

$$\mathrm{Ai}(x) \approx \frac{1}{\sqrt{\pi}(-x)^{1/4}} \sin\left(\frac{2}{3}(-x)^{3/2} + \frac{\pi}{4}\right), \tag{20}$$

valid for $x < -1.5$. Since the asymptotic expression (20) represents the Airy function above the first maximum with an accuracy of a few percentage points, one can easily obtain the position of the maxima and minima of the gross structure from the following equation valid for the detected electron energies higher than $\kappa^2/2$:

$$S(k) = -\left[\frac{3}{2}\left(\pi n \pm \frac{\pi}{4}\right)\right]^{2/3}, \quad n = 1,2,\ldots, \tag{21}$$

where the upper sign (+) corresponds to maxima, the lower sign (−) to minima. For the energies below $\kappa^2/2$ the same Eq. (21) is valid but for $\bar{S}(k)$.

Knowing the positions of the maxima of $|\mathrm{Ai}(S)|^2$ and using Eqs. (18) and (19), one can calculate the corresponding energy positions of the gross-structure maxima in the spectrum. (Note that for our choice of the IR pulse $\alpha \approx 0$.) In Fig. 1(d) we have shown by arrows the positions of the maxima calculated using Eq. (17). They agree very well with the maxima of the averaged spectra, calculated with Eq. (9). Importantly, the positions of the maxima of the gross structure depend on the IR field frequency and intensity but are independent of the parameters of the XUV pulse. Therefore, these maxima are at the same energy for all XUV pulse durations (see Fig. 1).

Analyzing expression (17), one can conclude that the gross structure is mainly localized in the k variable in the interval $[\kappa + \alpha - A_{0L}, \kappa + \alpha + A_{0L}]$ where its maxima and minima modulate the intensity of the conventional sideband lines,

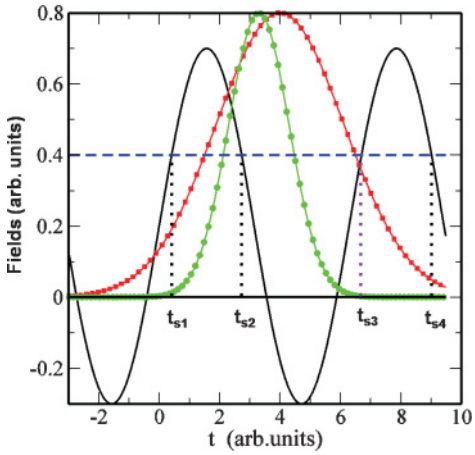

FIG. 2. (Color online) Schematic presentation of the fields and the positions of the stationary phase points t_s. Solid (black) line represents a part of the IR vector potential, lines with symbols show envelopes of two XUV pulses. Horizontal dashed line shows the value of $k - \kappa$. For further explanations see the text.

equidistant in the energy variable $k^2/2$. The same maxima and minima are responsible for the spectral structure at the XUV pulse duration $\tau_X \leqslant T_L$ [see Fig. 1(a)].

The presented analysis is valid for the pulses of approximately rectangular shape (with a flat middle part). However, our conclusions are valid for the pulses of arbitrary shape. All the above-mentioned properties of the spectra can be qualitatively obtained using the following simple "rules:"

(i) The main contribution to the spectra comes from the vicinities of stationary phase points t_s [see Eq. (16) and Fig. 2].

(ii) The magnitude of the contribution from a stationary point is proportional to the XUV pulse strength at this point.

(iii) If more than one stationary phase points contribute, their contributions interfere.

(iv) If the stationary points are close, the Airy function representation, Eq. (17), describes well their contribution.

From these rules it follows that if the XUV pulse is very short (green curve with dots in Fig. 2), only one of the stationary points (t_{s2} in Fig. 2) contributes substantially. This case corresponds to the streaking picture with one maximum in the spectrum. When three or more stationary points are covered by the XUV pulse (red curve with squares in Fig. 2), one has a complicated picture of interference between the contributions of all the stationary points involved (t_{s1}–t_{s4}) with one of them giving the dominant contribution (in Fig. 2 this point is t_{s2}). From this qualitative consideration it follows that the positions of minima and maxima in the electron spectrum are, as a rule, rather robust since they are determined by the phase shift between the fixed stationary points. (In some cases, when the extrema are not pronounced, this rule can fail.)

In the above calculations it was supposed that both IR and XUV pulses are phase stabilized. Since in real experiments it may be not the case, it is of interest to investigate how the calculated spectra depend on the relative delay time of the pulses. In Fig. 3 we show the results for the 1 fs [Fig. 3(a)] and 2 fs [Fig. 3(b)] XUV pulses calculated for different delay times between the XUV and IR pulses within one period of the IR light. Note that we define the delay $\Delta t = 0$ if the

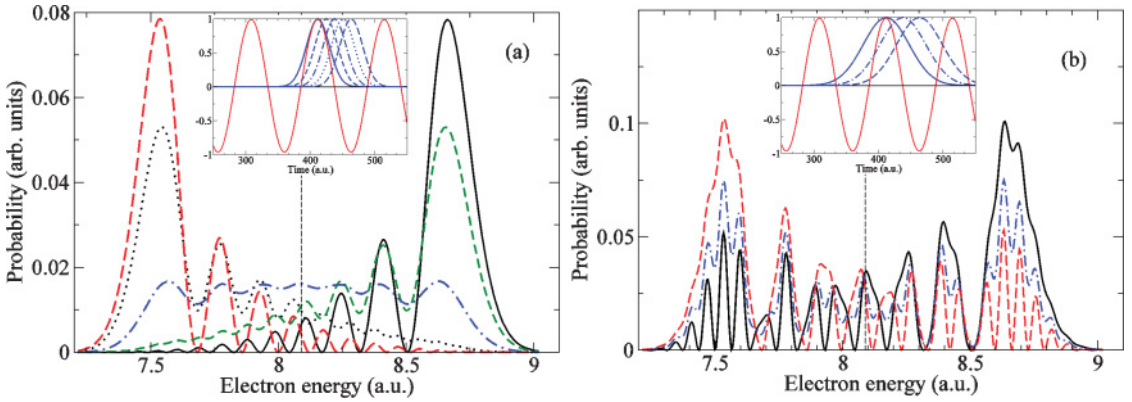

FIG. 3. (Color online) The calculated electron spectra excited by the XUV pulses of durations [(a) 1 fs and (b) 2 fs] for different delay times within one laser period. Solid line $\Delta t = 0$, short-dashed line $\Delta t = T_L/8$, dash-dotted line $\Delta t = T_L/4$, dotted line $\Delta t = 3T_L/8$, long-dashed line $\Delta t = T_L/2$. In the inset the corresponding lines show the position of the XUV-pulse envelope relative to the IR vector potential. Other parameters of the pulses are the same as in Fig. 1. Dashed vertical line shows the position of the unperturbed photoline.

XUV-pulse maximum coincides with the maximum of the IR vector potential (see the inserts in Fig. 3). In the case of a very short XUV pulse [Fig. 3(a)] the streaking effect dominates, and the spectrum strongly varies with the delay. Interesting that at $\Delta t = T_L/4$ the spectral maximum is almost completely washed out. In the case of a longer XUV pulse [Fig. 3(b)] the streaking effect is not so pronounced albeit visible. Importantly, the positions of the main maxima and minima (maxima and minima of the gross structure) are very stable and independent of the delay time. Thus the gross structure of the sidebands should preserve even for phase nonstabilized pulses. This follows also from the qualitative discussion above.

B. Photoelectron angular distributions

The angular distribution of photoelectrons is axially symmetrical with respect to the z axis (joint direction of the IR and XUV light polarizations). The dependence on the polar angle ϑ is determined by two factors: first, the angular distribution of photoelectrons without IR field, Eq. (6), and, second, the angular dependence of the emitted electron interaction with the IR field, Eq. (3). In the case of the s subshell ionization, the first factor gives $\cos^2\vartheta$ dependence with zero emission probability at $\vartheta = 90^\circ$. The effect of the second factor drastically depend on the duration of the XUV pulse and on the delay between the two pulses.

As an illustration, in Fig. 4 we show the calculated energy-angular distributions of photoelectrons (double differential cross section) for three different durations of the XUV pulse: (a) 1 fs, (b) 2 fs, and (c) 4 fs. The photoelectron energy (without IR field) is set equal to 220 eV. All other parameters are kept the same as in Fig. 1. The distributions are presented as two-dimensional color-scale plots. In all three panels the zero at 90° is clearly seen. For the shortest XUV pulse [1 fs, Fig. 4(a)] the angular distribution for any electron energy is strongly asymmetrical. For the strongest maximum this picture is close to the streaking one (see, for example, Ref. [29]). Additional maxima, which appear due to interference, are precursors of the sidebands. The spectrum changes dramatically with the angle.

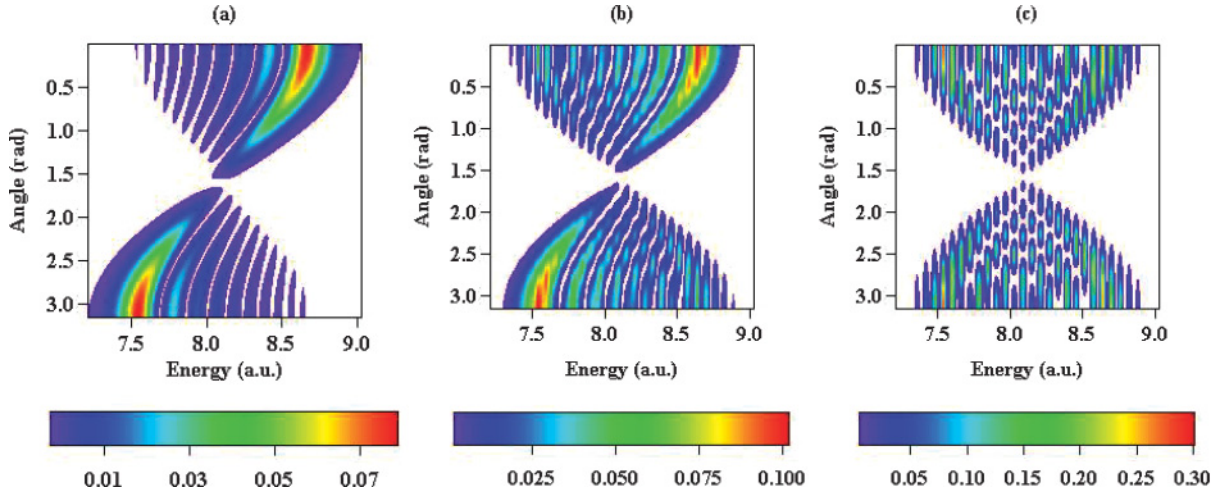

FIG. 4. (Color online) The calculated energy-angle distributions of photoelectrons for ionization of an s shell for different durations of the XUV pulse (a) 1 fs, (b) 2 fs, and (c) 4 fs. Other parameters are the same as in Fig. 1.

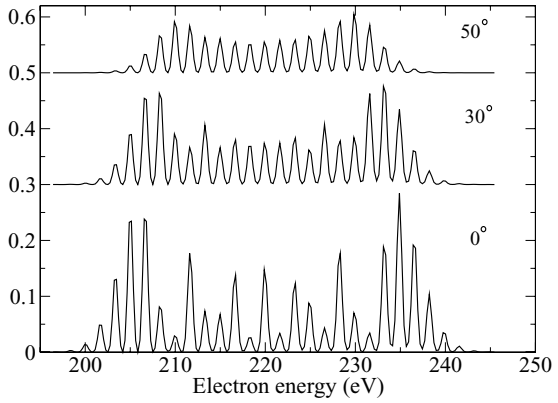

FIG. 5. The calculated photoelectron spectra of s subshell photoionization for different detection angles, indicated near the spectra. The XUV pulse duration is 4 fs. Other parameters are the same as in Fig. 1.

For a longer XUV pulse [2 fs, Fig. 4(b)], the sidebands have been partly formed, and the angular distribution becomes more symmetrical; however, the influence of streaking is still large. At the longest considered XUV pulse [4 fs, Fig. 4(c)], the angular distribution for each of the sidebands, which are close to the central maximum, contains in general several oscillations, which shows that higher powers of $\cos^2\theta$ contribute. For the sidebands which are far from the central maximum the angular distribution is sharply peaked at 0° and 180° without additional maxima in between.

In Fig. 5 we present the calculated spectra for some particular angles indicated near the curves. The calculations were performed for the 4 fs XUV pulse [compare with Fig. 4(c)]. For clearness, the spectra are shifted along the ordinate axis. To imitate the effect of acceptance angle in real experiment, we averaged the calculated spectra over the angles with the Gaussian weight of 15° width. One sees that in the forward direction (0°) the spectrum contains many sidebands with clearly seen gross structure. When the observation angle increases toward 90°, the spread of

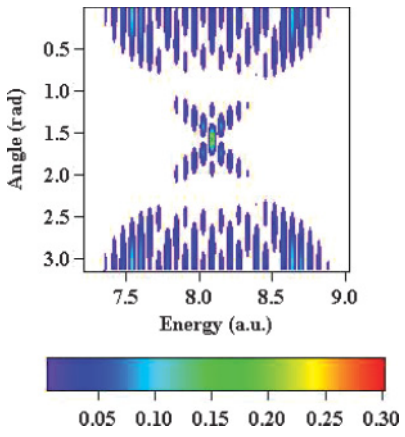

FIG. 6. (Color online) The calculated angle-energy distribution of photoelectrons for primary ionization of a $p(\sigma)$ electron into $d(\sigma)$ partial wave. The duration of the XUV pulse is 4 fs, the parameters of the laser pulse are the same as in Fig. 1.

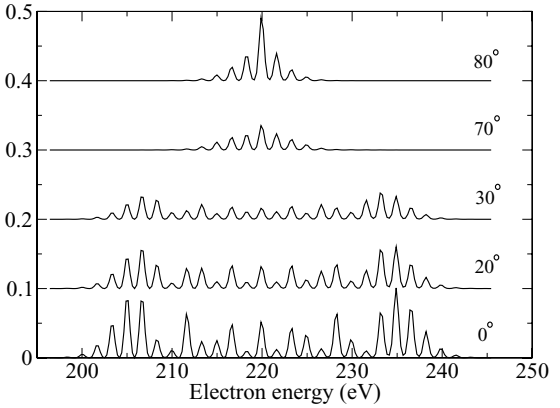

FIG. 7. The calculated photoelectron spectra for the primary ionization transition into the $d(\sigma)$ partial wave for different angles of detection, indicated near the spectra. The duration of the XUV pulse is 4 fs, the parameters of the laser pulse are the same as in Fig. 1.

the sidebands decreases and the gross structure gradually fades out.

It is instructive to consider the angular distributions for ionizations of subshells with nonzero orbital angular momentum, for example, of the p subshell. In this case, the ionized electron leaves the atom as an s or d wave. The case of an outgoing s wave interacting with the IR field has been considered in our articles [31–33]. Here we show the results for the d wave. Figure 6 shows the energy-angular distribution of emitted electrons for ionization from $p(\sigma)$ state, i.e., the projection of orbital angular momentum onto the z axis is zero. The XUV pulse duration is 4 fs. The angular distributions differ drastically from the previous case of s subshell ionization [compare with Fig. 4(c)]. Instead of zero at 90° one has a maximum. But there are two deep "valleys" at about 55° and 125° in the angular distribution of each sideband which are determined by the zeros of the spherical function $Y_{20}(\cos\vartheta)$. In Fig. 7 the spectra of photoelectrons are shown for different detection angles. As in the previous case, the well-developed gross structure is clearly seen at small angles (similarly, at large angles, close to 180°). It gradually fades out outside these regions. The sideband spectrum becomes narrower with increasing angle. Closer to 90° the character of the spectrum changes radically. One can see the big central maximum surrounded by small number of weak sidebands.

IV. CONCLUSION

We have investigated the transition from the streaking to the sideband regime in the angle-resolved spectra of photoelectrons produced by a short XUV pulse in the presence of a strong laser field. For a large energy of photoelectrons the sidebands reveal the gross structure, i.e., the modulation of the intensity of the sideband lines. This modulation is most pronounced at observation angles close to the direction of the light polarization. The gross structure is well described by the analytical expression involving the Airy function. Both the conventional sidebands and their gross structure are related to the properties of the pulses. Specific properties of the

ionized atom are substantially masked in the studied spectra by the universal sideband structure. Therefore, in the planning of any two-color XUV + IR experiment for studying the photoionization dynamics, the existence of the sidebands has to be taken into account. On the other hand, the study of the sidebands and their structure can be used for the investigation of the properties of the pulses.

ACKNOWLEDGMENTS

The authors are grateful to M. Meyer for numerous useful discussions and for critical reading of the manuscript and to K. Ueda for stimulating discussions. N.M.K. is grateful to Hamburg University and to Donostia International Physics Center (DIPC) for hospitality and for the financial support.

[1] A. Maquet and R. Taïeb, J. Mod. Opt. **54**, 1847 (2007).
[2] M. Meyer *et al.*, Phys. Rev. A **74**, 011401(R) (2006).
[3] J. Mauritsson, P. Johnsson, R. López-Martens, K. Varjú, W. Kornelis, J. Biegert, U. Keller, M. B. Gaarde, K. J. Schafer, and A. L'Huillier, Phys. Rev. A **70**, 021801(R) (2004).
[4] J. Itatani, F. Quéré, G. L. Yudin, M. Yu. Ivanov, F. Krausz, and P. B. Corkum, Phys. Rev. Lett. **88**, 173903 (2002).
[5] M. Kitzler, N. Milosevic, A. Scrinzi, F. Krausz, and T. Brabec, Phys. Rev. Lett. **88**, 173904 (2002).
[6] M. Hentschel, R. Kienberger, Ch. Spielmann, G. A. Reider, N. Milosevic, T. Brabec, P. Corkum, U. Heinzmann, M. Drescher, and F. Krausz, Nature (London) **414**, 509 (2001).
[7] G. Sansone *et al.*, Science **314**, 443 (2006).
[8] E. Gouliemakis *et al.*, Science **320**, 1614 (2008).
[9] U. Frühling *et al.*, Nature Photon. **3**, 523 (2009).
[10] P. M. Paul, E. S. Toma, P. Breger, G. Mullot, F. Augé, Ph. Balcou, H. G. Muller, and P. Agostini, Science **292**, 1689 (2001).
[11] R. López-Martens *et al.*, Phys. Rev. Lett. **94**, 033001 (2005).
[12] T. E. Glover, R. W. Schoenlein, A. H. Chin, and C. V. Shank, Phys. Rev. Lett. **76**, 2468 (1996).
[13] E. S. Toma, H. G. Muller, P. M. Paul, P. Breger, M. Cheret, P. Agostini, C. Le Blanc, G. Mullot, and G. Cheriaux, Phys. Rev. A **62**, 061801(R) (2000).
[14] P. O'Keeffe, R. Lopez-Martens, J. Mauritsson, A. Johansson, A. L'Huillier, V. Véniard, R. Taïeb, A. Maquet, and M. Meyer, Phys. Rev. A **69**, 051401(R) (2004).
[15] M. Meyer *et al.*, Phys. Rev. Lett. **101**, 193002 (2008).
[16] A. Cionga, V. Florescu, A. Maquet, and R. Taïeb, Phys. Rev. A **47**, 1830 (1993).
[17] V. Véniard, R. Taïeb, and A. Maquet, Phys. Rev. Lett. **74**, 4161 (1995).
[18] V. Véniard, R. Taïeb, and A. Maquet, Phys. Rev. A **54**, 721 (1996).
[19] O. Guyétand *et al.*, J. Phys. B **38**, L357 (2005).
[20] O. Guyétand *et al.*, J. Phys. B **41**, 051002 (FT) (2008).
[21] S. A. Aseyev, Y. Ni, L. J. Frasinski, H. G. Muller, and M. J. J. Vrakking, Phys. Rev. Lett. **91**, 223902 (2003).
[22] K. Varjú *et al.*, J. Phys. B **39**, 3983 (2006).
[23] P. Emma *et al.*, Nature Photon. **4**, 641 (2010).
[24] Y. Ding *et al.*, Phys. Rev. Lett. **102**, 254801 (2009).
[25] L. V. Keldysh, Sov. Phys. JETP **20**, 1307 (1965).
[26] A. K. Kazansky and N. M. Kabachnik, J. Phys. B **39**, 5173 (2006).
[27] O. Smirnova, M. Spanner, and M. Yu. Ivanov, J. Phys. B **39**, S323 (2006).
[28] O. Smirnova, A. S. Mouritzen, S. Patchkovskii, and M. Yu. Ivanov, J. Phys. B **40**, F197 (2007).
[29] A. K. Kazansky and N. M. Kabachnik, J. Phys. B **40**, 2163 (2007).
[30] A. K. Kazansky and N. M. Kabachnik, J. Phys. B **40**, 3413 (2007).
[31] A. K. Kazansky and N. M. Kabachnik, J. Phys. B **42**, 121002 (2009).
[32] A. K. Kazansky, I. P. Sazhina, and N. M. Kabachnik, J. Phys. B **42**, 245601 (2009).
[33] A. K. Kazansky and N. M. Kabachnik, J. Phys. B **42**, 035601 (2009).
[34] J. M. Schins, P. Breger, P. Agostini, R. C. Constantinescu, H. G. Muller, G. Grillon, A. Antonetti, and A. Mysyrowicz, Phys. Rev. A **52**, 1272 (1995).
[35] M. Lewenstein, P. Balcou, M. Y. Ivanov, A. L'Huillier, and P. B. Corkum, Phys. Rev. A **49**, 2117 (1994).
[36] F. Quéré, Y. Mairesse, and J. Itatani, J. Mod. Opt. **52**, 339 (2005).
[37] L. D. Landau and E. M. Lifshitz, *Quantum Mechanics: Non-relativistic Theory* (Pergamon, New York, 1979).
[38] D. V. Volkov, Z. Phys. **94**, 250 (1935).
[39] H. R. Reiss, Phys. Rev. A **22**, 1786 (1980).
[40] *Handbook of Mathematical Functions*, edited by M. Abramowitz and I. A. Stegun (NBS, Washington, D.C., 1972).